Journal of ELECTRONIC MATERIALS, Vol. 46, No. 1, 2017
DOI: 10.1007/s11664-016-4898-2

Good Thermal Stability, High Permittivity, Low Dielectric Loss and Chemical Compatibility with Silver Electrodes of Low-Fired $BaTiO_3$–$Bi(Cu_{0.75}W_{0.25})O_3$ Ceramics

XIULI CHEN,[1] DANDAN MA,[1] JIE CHEN,[1] GUISHENG HUANG,[1] and HUANFU ZHOU[1,2]

1.—Collaborative Innovation Center for Exploration of Hidden Nonferrous Metal Deposits and Development of New Materials in Guangxi, Guangxi Ministry-Province Jointly-Constructed Cultivation Base for State Key Laboratory of Processing for Non-ferrous Metal and Featured Materials, Guangxi Key Laboratory in Universities of Clean Metallurgy and Comprehensive Utilization for Non-ferrous Metals Resources, School of Materials Science and Engineering, Guilin University of Technology, Guilin 541004, China. 2.—e-mail: zhf_032@163.com

$(1 - x)BaTiO_3$–$xBi(Cu_{0.75}W_{0.25})O_3$ [$(1 - x)$BT–xBCW, $0 \le x \le 0.04$] perovskite solid solutions ceramics of an X8R-type multilayer ceramic capacitor with a low sintering temperature (900°C) were synthesized by a conventional solid state reaction technique. Raman spectra and x-ray diffraction analysis demonstrated that a systematically structural evolution from a tetragonal phase to a pseudo-cubic phase appeared near $0.03 < x < 0.04$. X-ray photoelectron analysis confirmed the existence of Cu^+/Cu^{2+} mixed-valent structure in 0.96BT–0.04BCW ceramics. 0.96BT–0.04BCW ceramics sintered at 900°C showed excellent temperature stability of permittivity ($\Delta\varepsilon/\varepsilon_{25°C} \le \pm 15\%$) and retained good dielectric properties (relative permittivity ~1450 and dielectric loss ≤2%) over a wide temperature range from 25°C to 150°C at 1 MHz. Especially, 0.96BT–0.04BCW dielectrics have good compatibility with silver powders. Dielectric properties and electrode compatibility suggest that the developed materials can be used in low temperature co-fired multilayer capacitor applications.

Key words: $BaTiO_3$, low-fired, X8R

INTRODUCTION

Perovskite dielectric materials with a high relative permittivity and good thermal stability for multilayer ceramic capacitor (MLCC) applications have been extensively researched.[1–4] Generally, some noble metals, such as Pt, Au, and Pd, were used as the internal electrode, which much increased the cost of MLCCs devices. If the sintering temperature can be reduced to ≤900°C, Ag could be used as the internal electrode, which is much cheaper than Pt, Au, and Pd.[5] In this case, much attention has been paid to developing materials with low sintering temperature to reduce the cost of MLCCs products, high relative permittivity to minimize the size of components, and good thermal stability to maintain the accuracy of devices.

Due to high relative permittivity and low dielectric loss, $BaTiO_3$-based dielectric ceramics have been extensively studied for capacitor applications, especially for X8R-type MLCCs, such as $BaTiO_3$–$Na_{0.5}Bi_{0.5}TiO_3$–Nb_2O_5–NiO,[6] $BaTiO_3$–Mn_3O_4–$Bi_4Ti_3O_{12}$,[7] $BaTiO_3$–Nb_2O_5–Co_2O_3–Sm_2O_3–CeO_2–$Bi(Mg_{0.5}Ti_{0.5})O_3$,[3] $BaTiO_3$–$Bi(Mg_{2/3}Ta_{1/3})O_3$,[9] $BaTiO_3$–MgO–MnO_2–Y_2O_3–$CaZrO_3$,[10] and $BaTiO_3$–$MgCO_3$–$MnCO_3$–$BaSiO_3$,[11] $BaTiO_3$–$Bi(Mg_{2/3}Nb_{1/3})O_3$.[12] However, high sintering temperatures (≥1200°C) restrict their further applications in MLCCs devices using low cost metals for electrodes. So it is very important to reduce the sintering temperatures of $BaTiO_3$-based materials. In general, there are two methods to reduce

(Received May 7, 2016; accepted August 19, 2016; published online September 2, 2016)

the sintering temperature of materials,[13–17] including the addition of low-melting sintering aids and ultrafine powder prepared by chemical processing or advanced synthesis processing, such as hydrothermal, oxalic, and sol–gel. For the first method, the dielectric performance could be degraded seriously by adding large amounts of sintering aids. The second approach would induce the complex procedure, which increases the cost of devices. As for $BaTiO_3$-based materials, much work has been done to reduce the sintering temperature (>1300°C). Hsiang et al.[18] utilized glass addition to reduce the sintering temperature of BT material. However, the relative permittivity of ceramics can also be reduced to <1000. Tian et al.[19] investigated the $BaTiO_3$-based X7R ceramics by a chemical coating method. These materials could be sintered at 950°C, but a complicated procedure restricts their further applications. Recently, Zhang et al.[20] reported that $BaTiO_3$–$Bi(Mg_{1/2}Ti_{1/2})O_3$ has a stable permittivity (~1500) and low loss ($\tan\delta < 2\%$), but high sintering temperature (1100°C)and is not suitable to using Ag as the internal electrode.

In this paper, $Bi(Cu_{0.75}W_{0.25})O_3$ perovskite compound was introduced to a $BaTiO_3$ matrix to form $(1-x)BaTiO_3$–$xBi(Cu_{0.75}W_{0.25})O_3$ [$(1-x)$BT–xBCW, $0 \le x \le 0.04$] solid solutions. The sintering ability, phase evolution, microstructure, and dielectric properties of ceramics were studied. Furthermore, the chemical compatibility between the 0.96BT–0.04BCW ceramics and Ag was also investigated. The aim of this work was to develop a low-fired material.

EXPERIMENTAL

$(1-x)$BT–xBCW ($0 \le x \le 0.04$) ceramics samples were prepared via the conventional solid state reaction technique. Carbonates and oxides were used as the main raw powders, including $BaCO_3$ (≥99%, Guo-Yao Co. Ltd, Shanghai, China), TiO_2 (≥99.99%, Guo-Yao Co. Ltd, Shanghai, China), Bi_2O_3 (≥99%, Guo-Yao Co. Ltd, Shanghai, China), CuO (≥99%, Guo-Yao Co. Ltd, Shanghai, China) and WO_3 (≥99%, Guo-Yao Co. Ltd, Shanghai, China). Stoichiometric ratios of BT and BCW were mixed in alcohol medium using zirconia balls for 4 h. The slurries were dried and then calcined at 1100°C and 600°C for 4 h, respectively. Subsequently, $(1-x)$BT–xBCW ($0 \le x \le 0.04$) powders were weighed and milled in alcohol medium using zirconia balls for 4 h. After drying, the resultant powders were mixed with 5 wt.% of polyvinyl alcohol (PVA) and pressed into pellets with 12 mm diameters and ~2 mm thicknesses. The compacted pellets were sintered with an embedded sintering method in closed alumina crucibles: pellets were embedded with the calcined powders of the same composition to minimize alkaline elements volatilization and sintered at different temperatures, depending on the content of BCW, ranging from 900°C to 1350°C for 2 h in air.

The crystal structures of the ceramics were measured by an x-ray diffractometer (XRD) (CuKα1, 1.54059 Å, Model X'Pert PRO, PANalytical, Almelo, Holland) operated at 40 kV and 40 mA with a 2θ scan speed of 1°/min. The phase analysis for the XRD data was performed by PanAlytical software (X'Pert Highscore Plus). Raman spectroscopy was carried out on a Thermo Fisher Scientific DXR using a 10 mW laser with a wavelength of 532 nm. The microstructural observation of the samples was performed using a field emission scanning electron microscope (FE-SEM, Model S4800, Hitachi, Japan). Composition analysis was performed using energy-dispersive spectroscopy (EDS, IE 350; INCA, Oxford, UK). The chemical bonding states of the ceramics were investigated by x-ray photoelectron spectroscopy (XPS, Model ESCALAB250, Thermo Fisher Scientific). Silver electrodes were coated on both sides of the pellets, and then fired at 650°C for 30 min. Dielectric properties were measured with an applied voltage of 500 mV over 100 Hz–1 MHz from room temperature to 500°C using a precision impedance analyzer (Model 4294A, Hewlett-Packard Co., Palo Alto, CA) at a heating rate of 3°C/min.

RESULTS AND DISCUSSION

Figure 1a shows the room temperature x-ray diffraction (XRD) patterns of BT–BCW samples in 2θ=20°–60°. A single perovskite phase is formed and no secondary phases are observed, which indicates that $Bi(Cu_{0.75}W_{0.25})O_3$ has fully diffused into the lattice of $BaTiO_3$ and formed a homogeneous solid solution. The merging of (002)/(200) diffraction peaks into a single (200) peak was near the compositions of $0.03 < x < 0.04$, indicating a transformation from tetragonal phase ($P4mm$) to pseudo-cubic symmetry.[21,22] In our previous work,[2] $BaTiO_3$–$Bi(Mg_{0.75}W_{0.25})O_3$ solid solutions showed good dielectric temperature stability over a wide temperature range from 200°C to 500°C for thermal stability device applications. Based on the above analysis, the substitution of an A-site ion Ba^{2+} (1.61 Å) by Bi^{3+} ($1.03\ Å < r_{Bi}^{3+} < 1.61$ Å) and/or a B-site ion Ti^{4+} (0.604 Å) by $^2Mg^+$ (0.72 Å), and W^{6+} (0.6 Å) can tailor the dielectric properties of BT. Considering the identical valence and similar ionic radius of Mg^{2+} and Cu^{2+} (0.73 Å), we could anticipate that the substitution of an A-site by Bi^{3+} and/or a B-site by Cu^{2+} (0.72 Å), and W^{6+} (0.6 Å). The profile fits of the Rietveld refinement for x = 0.04 are shown in Fig. 1b, and the refined structural parameters are listed in Table I. It can be seen that Bi ions rightly enter the lattice site for Ba (1a), while Cu and W ions enter the lattice site for Ti (1b), which is consistent with the expected result.

Room temperature Raman spectra for $(1-x)$BT–xBCW ($0 \le x \le 0.04$) ceramics are used to get a better illustration of the phase evolution, as shown in Fig. 1c. The vibrational modes considered for this work are indexed in the diagram. Based on

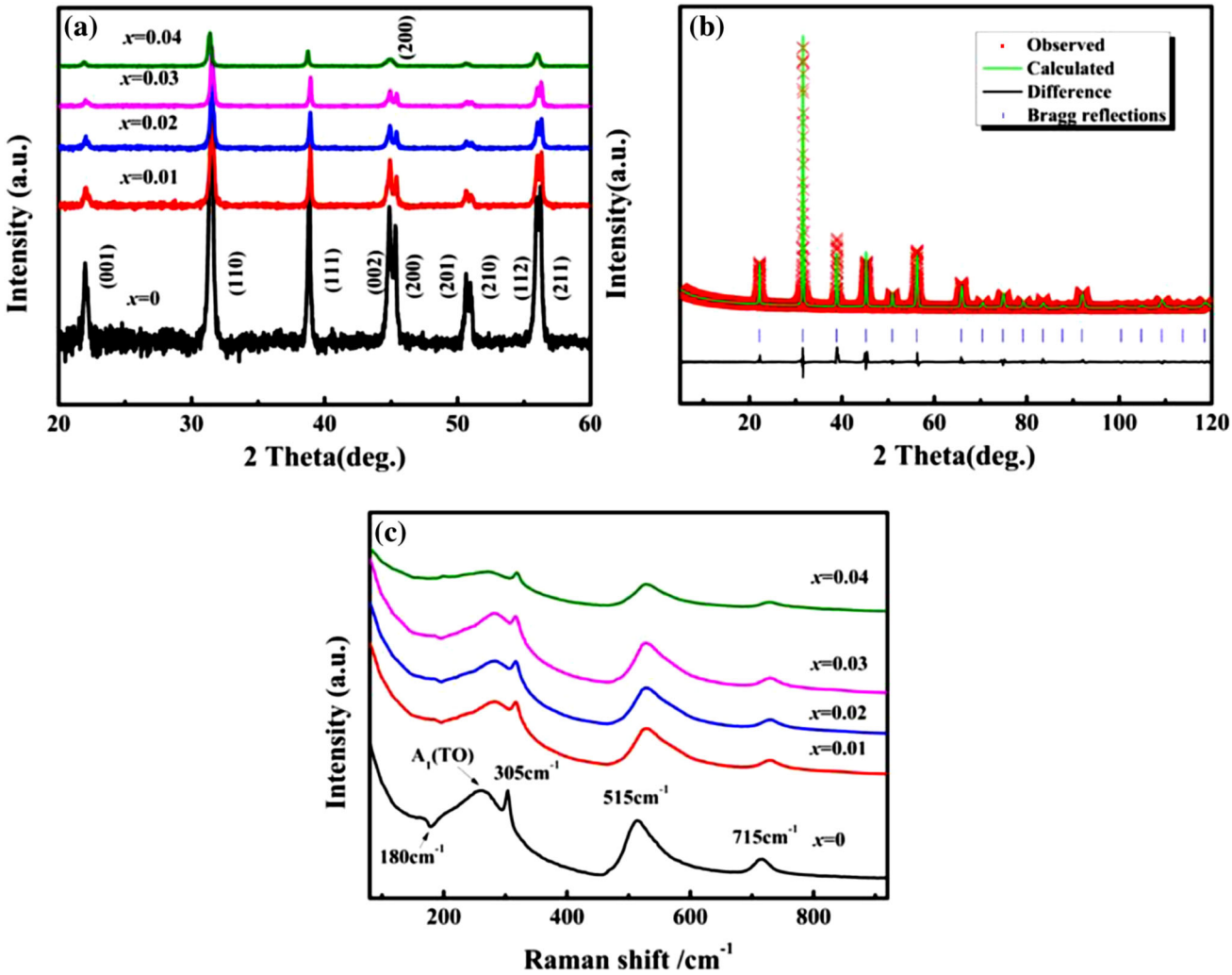

Fig. 1. (a) X-ray diffraction patterns of $(1 - x)$BT–xBCW ($0 \le x \le 0.04$) ceramics, (b) Rietveld refinement for 0.96BT–0.04BCW ceramic at room temperature, (c) Room temperature Raman spectra of $(1 - x)$BT–xBCW ceramics for x = 0, 0.01, 0.04, 0.06, 0.08, and 0.1 compositions.

Table I. Refined structure parameters for 0.96BT–0.04BCW ceramics

Atom	Site	x	y	z	Occupies	Biso (Å^2)
Ba1	1a	0	0	0	0.961 (2)	0.28 (3)
Bi1	1a	0	0	0	0.039 (1)	0.28 (3)
Ti1	1b	0.5	0.5	0.5	0.962 (1)	0.58 (1)
Cu1	1b	0.5	0.5	0.5	0.0294 (2)	0.58 (1)
W1	1b	0.5	0.5	0.5	0.0104 (3)	0.58 (1)
O1	3c	0	0.5	0.5	1	0.46 (2)

Lattice parameters: a = 4.00952 (7) Å, space group Pm-3m. Agreement indices: $R_{wp}(\%)$ = 8.39, $R_p(\%)$ = 4.51, $R_b(\%)$ = 2.28.

Pokorny's work,[23] the modes for x = 0 were assigned as a single crystal $BaTiO_3$. The Raman spectrum of pure tetragonal $BaTiO_3$ was characterized by an interference dip at ~180 cm^{-1}, a "silent" mode at ~305 cm^{-1}, asymmetric broader bands at A_1(TO) (~270 cm^{-1}), 515 cm^{-1} and the high-frequency modes at around 715 cm^{-1}.[24] A sharp dip at ~180 cm^{-1} emerges only in the presence of a long-range ferroelectric phase,[25,26] which matches well with the previous reports.[27–31] It is obviously observed that the resonance dip at ~180 cm^{-1} emerged in x = 0–0.03. With increasing the BCW content, the reduction in 715 cm^{-1} peak implied the decrease in tetragonality (c/a) and the destruction of

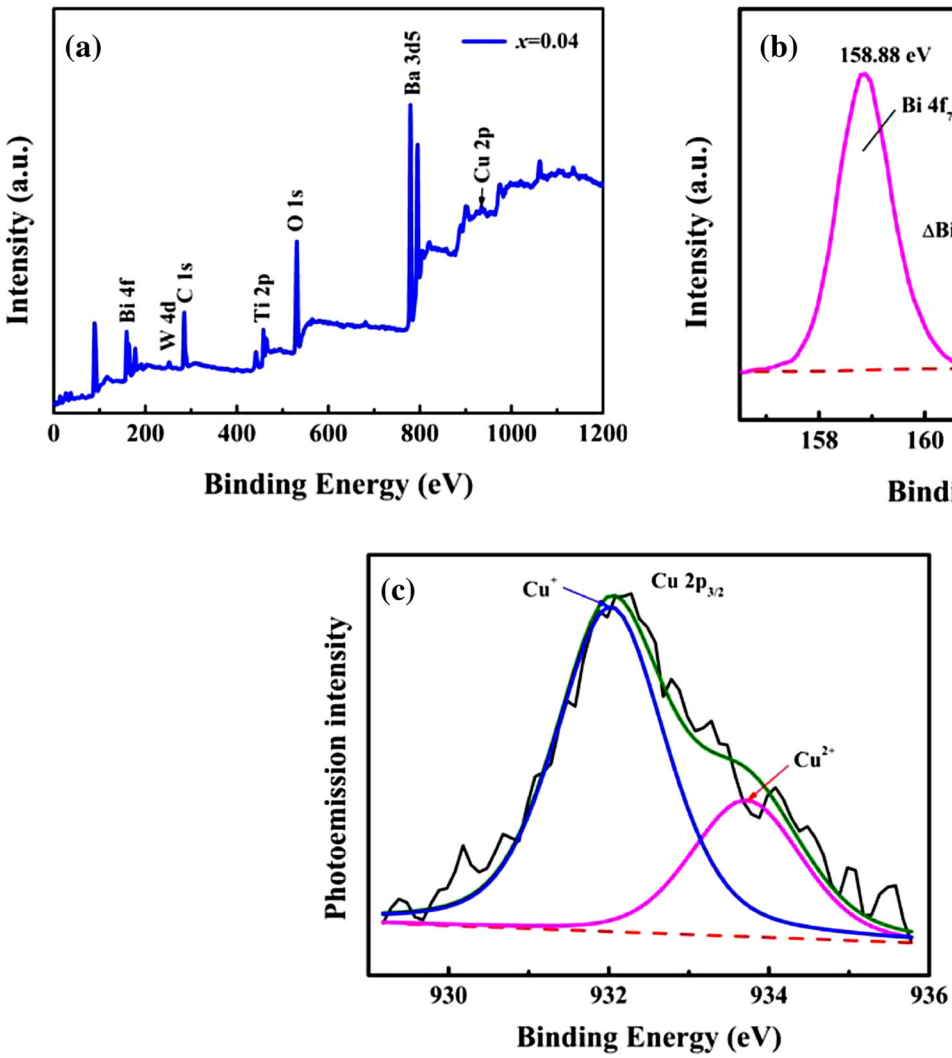

Fig. 2. (a) XPS survey spectra of 0.96BT–0.04BCW ceramics, (b) High-resolution XPS spectra of the Bi 4*f* core level, (c) High-resolution XPS spectra of the Cu 2*p* region.

the long-range ferroelectric order. It is clearly seen that the characteristic of long-range ferroelectric ordering in $BaTiO_3$ is absent in pseudocubic phases as x increases to 0.04. These results are consistent with the structure evaluation for the XRD patterns (Fig. 1a).

XPS analysis was carried out to investigate the oxidation states of polyvalent ions in 0.96BT–0.04BCW ceramics. The survey spectrum of 0.96BT–0.04BCW certified that the sample contains Ba, Ti, Bi, Cu, W, O, and C elements, as shown in Fig. 2a. C and part of O are adsorbed from the atmosphere. All peaks have been calibrated with respect to the C 1*s* peak at 284.8 eV. Figure 2b demonstrates the fitted narrow-scan spectra of the Bi 4*f* core level of the 0.96BT–0.04BCW compound. The Bi 4*f* doublet consists of two peaks at 158.88–164.18 eV, which is mainly identified as a signal of Bi($4f_{7/2}$)–O and Bi($4f_{5/2}$)–O bonds, respectively.[32] The spin–orbit splitting energy (Δ) of the Bi 4*f* doublet is 5.3 eV, which accords well with the theoretical value (5.31 eV).[33] The binding energy value connected with the Bi $4f_{7/2}$ peak is below 159.0 eV, which is a characteristic of Bi(III) in an oxide chemical state,[33,34] indicating that the valence state of Bi ions in 0.96BT–0.04BCW composition is trivalent. Figure 2c displays the XPS spectra of the Cu $2p_{3/2}$ region for 0.96BT–0.04BCW ceramics. The $2p_{3/2}$ peak for Cu can be split into two peaks by Gaussian–Lorentzian curve fitting, which shows the existence of Cu^+ with lower (932.02 eV) binding energy. The binding energy for each different valent ion is within the range of binding energies in the NIST XPS database, and the difference of FWHM between Cu^+ and Cu^{2+} peaks is <1. From the above analysis, the valence state of Cu ions in 0.96BT–0.04BCW composition is the Cu^+/Cu^{2+} mixed-valent structure. This phenomenon is similar to $CaCu_3Ti_4O_{12}$ ceramics.[35] In this work, the substitution of Cu^{2+} for Ti^{4+} would form Cu''_{Ti}, which results in transformation of Cu^{2+} to Cu^+.

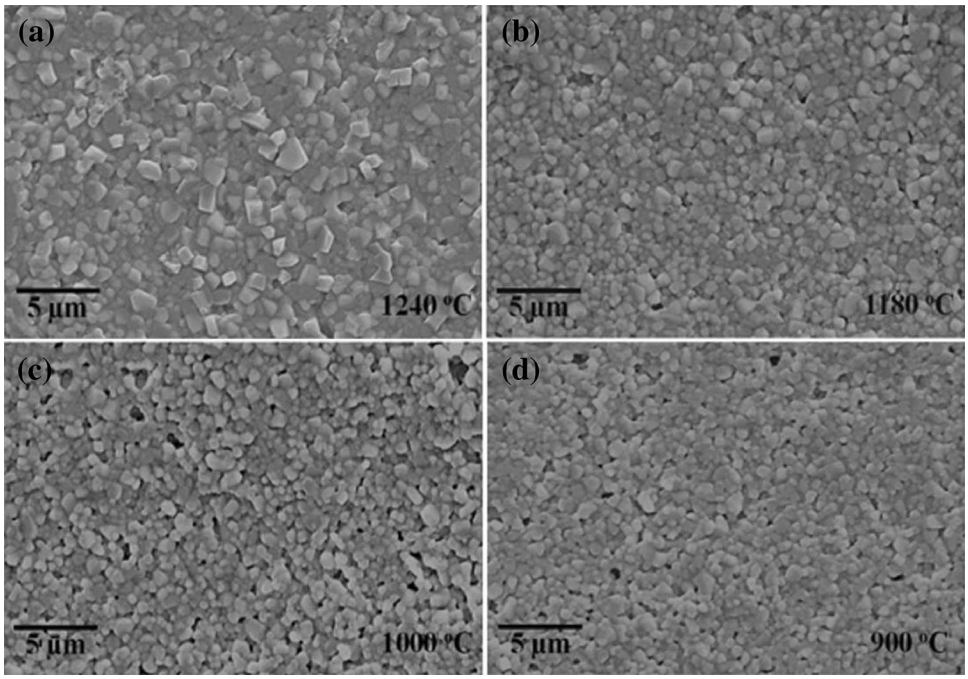

Fig. 3. SEM images of 0.96BT–0.04BCW ceramics sintered at different temperatures: (a) 1,240°C, (b) 1,180°C, (c) 1,000°C and (d) 900°C.

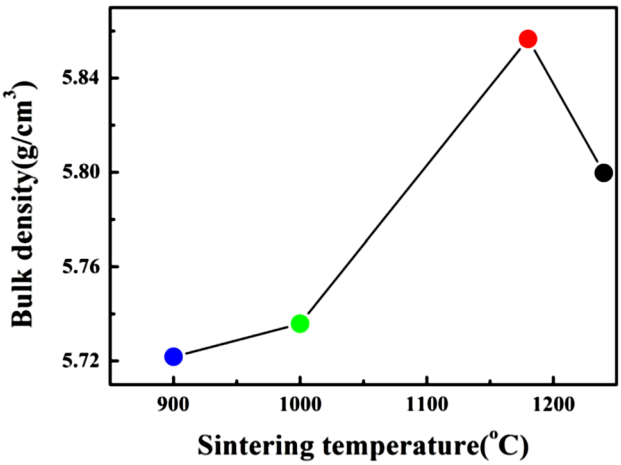

Fig. 4. Bulk density of 0.96BT–0.04BCW ceramics as a function of the sintering temperature.

The surface microstructures of a 0.96BT–0.04BCW compound sintered at different temperatures are demonstrated in Fig. 3a–d. It is clearly seen that the sintering temperature has a great effect on the average grain size. The average grain size of samples becomes smaller and uniform as the sintering temperature decreases from 1240°C to 1180°C, which implies that low sintering temperature may inhibit growth of grains. With further decreasing the sintering temperature (T = 900°C), the average grain size of a sample varies rarely, as shown in Fig. 3d. $Bi(Cu_{0.75}W_{0.25})O_3$ was added to $BaTiO_3$ to form a solid solution. The sintering temperature of the ceramics was reduced from 1350°C to 900°C because of the formation of a

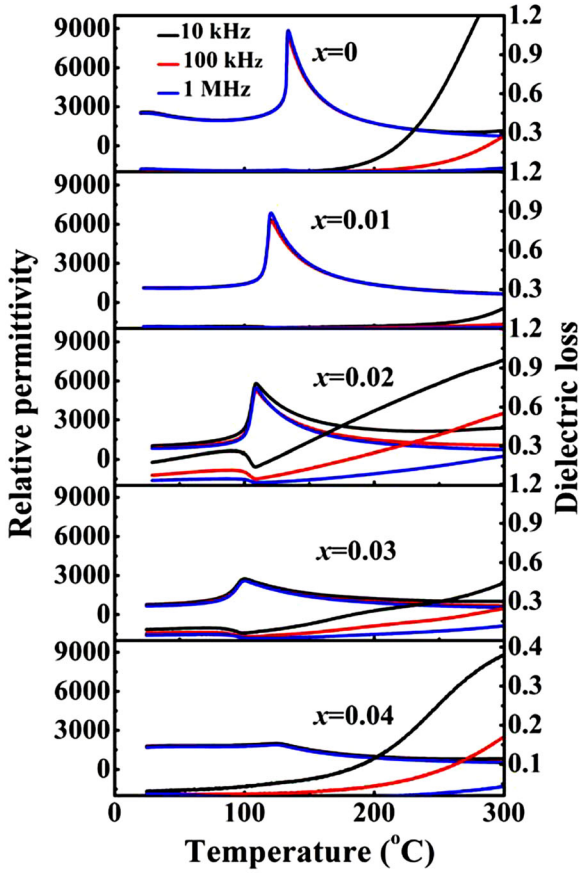

Fig. 5. Relative permittivity and dielectric loss as a function of temperature measured at frequencies from 10 kHz to 1 MHz for $(1 - x)$BT–xBCW ($0 \le x \le 0.04$).

$(1-x)BaTiO_3$–$xBi(Cu_{0.75}W_{0.25})O_3$ solid solution not in low melting phase in the grain boundary. So no other grain boundary phases were observed in the SEM pictures. Figure 4 shows the bulk density of 0.96BT–0.04BCW ceramics as a function of the sintering temperature. When the sintering temperature was increased from 900°C to 1240°C, the density of 0.96BT–0.04BCW ceramics increased firstly, reached a maximum value (~5.857 g/cm^3) as the sintering temperatures was increased to 1180°C, which is consistent with the SEM results.

Figure 5 demonstrates the temperature dependence of the relative permittivity and dielectric loss for $(1-x)$BT–xBCW ceramics (x = 0–0.04) measured at various frequencies (10 kHz–1 MHz). As shown in Fig. 5a, pure BT ceramics exhibit a reasonably sharp Curie peak, conforming to tetragonal-cubic phase transition, typical of a normal ferroelectric with Curie point, $T_c \sim 130$°C, which accords with the previous report.[36] It is obviously seen that the frequency dependence of dielectric property is weak. Figure 6 illustrates the temperature stability of permittivity ($\Delta\varepsilon/\varepsilon_{25°C}$), relative permittivity (ε_r) and dielectric loss (tanδ) for 0.96BT–0.04BCW ceramics with different sintering temperatures measured at 1 MHz. It is obviously seen that the composition possesses the optimum dielectric performance with small $\Delta\varepsilon/\varepsilon_{25°C}$ value (≤±15%) and high relative permittivity (~1450) over a broad temperature range from 25°C to 150°C as the sintering temperature changes from 900°C to 1240°C. Especially at 900°C, the loss tangent tanδ is ≤0.02. Table II lists the sintering

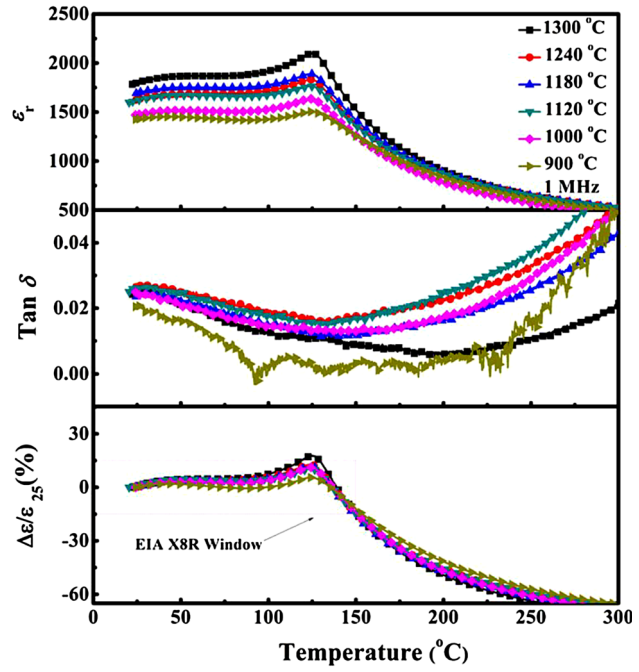

Fig. 6. The relative permittivity (ε_r), dielectric loss (tanδ), and $\Delta\varepsilon/\varepsilon_{25°C}$ as a function of temperature from 25°C to 300°C at 1 MHz for 0.96BT–0.04BCW ceramics sintered at 900–1300°C, where $\Delta\varepsilon = \varepsilon_{(25–300°C)} - \varepsilon_{25°C}$.

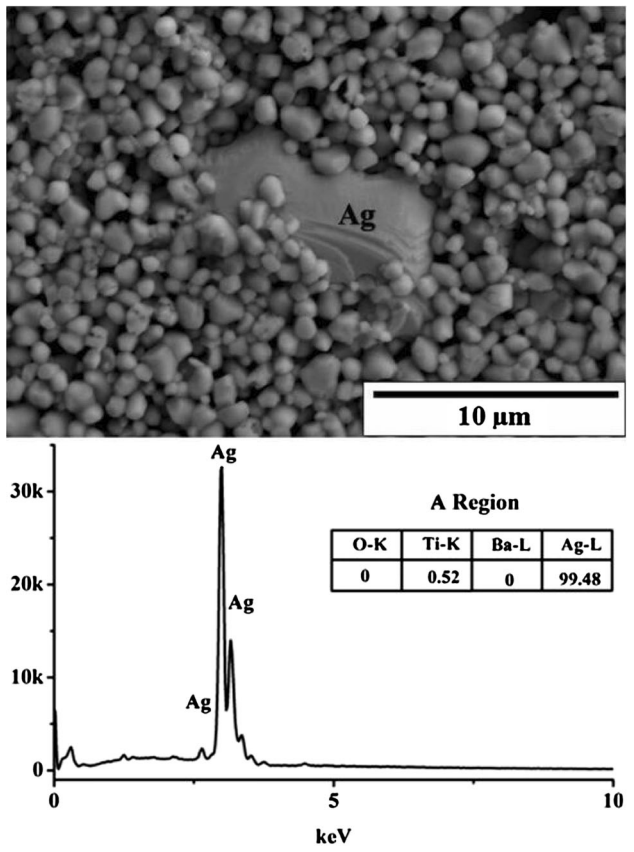

Fig. 7. BSEM image and EDS analysis of the 0.96BT–0.04BCW ceramics co-fired with 20 wt.% Ag.

Table II. Comparison of performance parameters of 0.96BT–0.04BCW with other barium titanate-based X8R ceramics

System	ε_r (25°C)	tanδ (25°C)	Sintering temperature (°C)	References
$BaTiO_3$–$Na_{0.5}Bi_{0.5}TiO_3$–Nb_2O_5–NiO	~2000	<0.025	1230	6
$BaTiO_3$–Nb_2O_5–Co_2O_3–Sm_2O_3–CeO_2–$Bi(Mg_{0.5}Ti_{0.5})O_3$	~1800	<0.015	1250	8
$BaTiO_3$–MgO–MnO_2–Y_2O_3–$CaZrO_3$	~2500	–	1311	10
$BaTiO_3$–$MgCO_3$–$MnCO_3$–$BaSiO_3$	–	–	1325	11
0.96$BaTiO_3$–0.04$Bi(Cu_{0.75}W_{0.25})O_3$	~1450	<0.02	900	This work

temperature, relative permittivity, and dielectric loss between our work and other $BaTiO_3$-based X8R ceramics. It is clearly seen that the sintering temperature (900°C) of 0.96BT–0.04BCW ceramics is significantly lower than other BT-based X8R dielectric materials, which indicates that the 0.96BT–0.04BCW ceramics could have a potential application for X8R-type capacitors using Ag as the internal electrode.

Back scattered electron micrograph (BSEM) image and energy dispersives spectrometer (EDS) analysis of the co-fired sample for the 0.96BT–0.04BCW ceramic with 20 wt.% Ag sintered at 900°C for 2 h are shown in Fig. 7. In the BSEM image, there are two distinct grains with different sizes observed. From the EDS analysis, the large grains were detected as Ag. This result indicated that 0.96BT-0.04BCW ceramics have good chemical compatibility with Ag.

CONCLUSIONS

$(1 - x)BaTiO_3$–$xBi(Cu_{0.75}W_{0.25})O_3$ $(x = 0–0.04)$ lead-free perovskite ceramics have been prepared by the solid state reaction method. The addition of $Bi(Cu_{0.75}W_{0.25})O_3$ could reduce the sintering temperature and improve the temperature stability of the $BaTiO_3$ ceramic. A $0.96BaTiO_3$–$0.04Bi(Cu_{0.75}W_{0.25})O_3$ ceramic sintered at 900°C exhibited high performance dielectric properties with a stable permittivity (~1450), small $\Delta\varepsilon/\varepsilon_{25°C}$ values (≤±15%), and lower dielectric loss (≤2%) over a broad temperature range from 25°C to 150°C. The 0.96BT–0.04BCW ceramic demonstrated good chemical compatibility with Ag when sintered at 900°C. All the results indicated that the 0.96BT–0.04BCW X8R ceramic is a promising material for low temperature co-fired multilayer capacitor applications.

ACKNOWLEDGEMENTS

This work was supported by the National Natural Science Foundation of China (Nos. 11664008, 11364012, and 11464009), the Natural Science Foundation of Guangxi (Nos. 2015GXNSFDA13 9033, 2014GXNSFAA118312, and 2014GXNSF AA118326), Research Start-up Funds Doctor of Guilin University of Technology (Nos. 002401003 281 and 002401003282), and the Project of Outstanding Young Teachers' Training in Higher Education Institutions of Guangxi.

REFERENCES

1. Y. Mizuno, T. Hagiwara, H. Chazono, and H. Kishi, *J. Eur. Ceram. Soc.* 21, 1649 (2001).
2. J. Chen, X.L. Chen, F. He, Y.L. Wang, H.F. Zhou, and L. Fang, *J. Electron. Mater.* 43, 1112 (2014).
3. Y. Wang, B. Cui, Y. Liu, X.T. Zhao, Z.Y. Hu, Q.Q. Yan, T. Wu, L.L. Zhao, and Y.Y. Wang, *Scr. Mater.* 90–91, 49 (2014).
4. C.K. Sun, X.H. Wang, C. Ma, and L.T. Li, *J. Am. Ceram. Soc.* 92, 1613 (2009).
5. D.H. Choi, A. Baker, M. Lanagan, S. Trolier-Mckinstry, and C. Randall, *J. Am. Ceram. Soc.* 96, 2197 (2013).
6. Y. Sun, H.X. Liu, H. Hao, Z. Song, and S.J. Zhang, *J. Am. Ceram. Soc.* 98, 1574 (2015).
7. T.A. Jain, C.C. Chen, and K.Z. Fung, *J. Eur. Ceram. Soc.* 29, 2595 (2009).
8. H. Hao, H.X. Liu, S.J. Zhang, B. Xiong, X. Shu, Z.H. Yao, and M.H. Cao, *Scr. Mater.* 67, 451 (2012).
9. D.D. Ma, X.L. Chen, G.S. Huang, J. Chen, H.F. Zhou, and L. Fang, *Ceram. Int.* 41, 7157 (2015).
10. G.F. Yao, X.H. Wang, T.Y. Sun, and L.T. Li, *J. Am. Ceram. Soc.* 94, 3856 (2011).
11. W.H. Lee and C.Y. Su, *J. Am. Ceram. Soc.* 90, 3345 (2007).
12. X.L. Chen, J. Chen, D.D. Ma, L. Fang, and H.F. Zhou, *J. Am. Ceram. Soc.* 98, 804 (2015).
13. M. Du, Y.R. Li, Y. Yuan, S.R. Zhang, and B. Tang, *J. Electron. Mater.* 36, 1389 (2007).
14. K.J. Zhu, J.H. Qiu, K. Kajiyoshi, M. Takai, and K. Yanagisawa, *Ceram. Int.* 35, 1947 (2009).
15. B. Tang, S.R. Zhang, X.H. Zhou, D. Wang, and Y. Yuan, *J. Electron. Mater.* 36, 1383 (2007).
16. W.G. Yang, B.P. Zhang, N. Ma, and L. Zhao, *J. Eur. Ceram. Soc.* 32, 899 (2012).
17. K.H. Lee, *J. Electron. Mater.* 44, 797 (2014).
18. H.I. Hsiang, C.S. Hsi, C.C. Huang, and S.L. Fu, *Mater. Chem. Phys.* 113, 658 (2009).
19. Z.B. Tian, H.B. Wang, L.K. Shu, T. Wang, T.H. Song, Z.L. Gui, and L.T. Li, *J. Am. Ceram. Soc.* 92, 830 (2009).
20. Q. Zhang, Z.R. Li, F. Li, and Z. Xu, *J. Am. Ceram. Soc.* 94, 4335 (2009).
21. K. Suzuki and K. Kijima, *J. Mater. Sci.* 40, 1289 (2005).
22. T. Li, K. Yang, R. Xue, Y. Xue, and Z. Chen, *J. Mater. Sci. Mater. Electron.* 22, 838 (2011).
23. J. Pokorny, U.M. Pasha, L. Ben, O.P. Thakur, D.C. Sinclair, and I.M. Reaney, *J. Appl. Phys.* 109, 114110 (2011).
24. U.D. Venkateswaran, V.M. Naik, and R. Naik, *Phys. Rev. B* 58, 14256 (1998).
25. R. Farhi, M.E. Marssi, A. Simon, and J. Ravez, *Eur. Phys. J. B* 9, 599 (1999).
26. A. Scalabrin, A.S. Chaves, D.S. Shim, and S.P.S. Porto, *Phys. Status Solidi B* 79, 731 (1977).
27. J.L. Parsons and L. Rimai, *Solid State Commun.* 5, 423 (1967).
28. M. DiDomenico Jr., S.H. Wemple, S.P.S. Porto, and R.P. Bauman, *Phys. Rev.* 174, 522 (1968).
29. N. Baskaran, A. Ghule, C. Bhongale, R. Murugan, and H. Chang, *J. Appl. Phys.* 91, 10038 (2002).
30. N.K. Karan, R.S. Katiyar, T. Maiti, R. Guo, and A.S. Bhalla, *J. Raman Spectrosc.* 40, 370 (2009).
31. U.M. Pasha, H. Zheng, O.P. Thakur, A. Feteira, K.R. Whittle, D.C. Sinclair, and I.M. Reaney, *Appl. Phys. Lett.* 91, 062908 (2007).
32. Z.C. Quan, W. Liu, H. Hu, S. Xu, B. Sebo, G.J. Fang, M.Y. Li, and X.Z. Zhao, *J. Appl. Phys.* 104, 084106 (2008).
33. J.K. Reddy, B. Srinivas, V.D. Kumari, and M. Subrahmanyam, *ChemCatChem* 1, 492 (2009).
34. K. Uchida and A. Ayame, *Surf. Sci.* 357, 170 (1996).
35. L. Ni and X.M. Chen, *Appl. Phys. Lett.* 91, 122905 (2007).
36. A. Zeb and S.J. Milne, *J. Eur. Ceram. Soc.* 34, 3159 (2014).